Mechanical Surface Treatment to Obtain Optically Cooperative Surfaces vis-à-vis Fringe Projection

Omar Abo-Namous[a] and Markus Kästner[a] and Eduard Reithmeier[a] and Martin Nicolaus[b] and Kai Möhwald[b] and Friedrich-Wilhelm Bach[b]

[a]Institute of Measurement and Automatic Control, Nienburger Str. 17, Hannover, Germany

[b]Institute of Materials Science, An der Universität 2, Garbsen, Germany

ABSTRACT

Fringe projection techniques are widely used for geometry measurement of synchro rings inside a manufacturing chain, since a dense areal geometrical data set is needed to evaluate all the key features. Post-process machined parts exhibit optically incooperative surfaces towards triangulation techniques. Hence these parts can't be measured accurately using fringe projection systems. The optical incooperativity originates from the scattering characteristics of the surface. Polished surfaces exhibit a narrow angle of light refraction, whereas rough surfaces scatter the light over a hemisphere more homogenously. The angle range at which an incident light ray is scattered is the basis for a definition of optical cooperativity. The wider the range, the higher is the optical cooperativity of the surface.

In order to produce optically cooperative surfaces of machined parts for the use of fringe projection measuring systems, we employ methods of surface treatment. One promising mechanical method under investigation to obtain optical cooperativity with technical surfaces is done by blasting the surface with fused alumina (EKF1000). The blasted surface leads to an increased roughness which can be controlled using the blast parameters, i.e. blast-pressure, blast-duration and the distance of the blaster to the part surface.

In this paper the effects of different parameters of the blast-process on the surface roughness, the optical roughness and on the optical cooperativity vis-à-vis fringe projection techniques are examined. Optimal parameter settings result in a sub-micrometer change with respect to the object surface. Since the effects due to a variation of the parameters are dependant on the object material, we restrict our research to the case-hardening steel 1.7193 (16MnCrS5).

Keywords: optical metrology, surface treatment, fringe projection, light scattering, optical cooperativity

1. INTRODUCTION

Fringe projection (FP) is a triangulatory geometry measurement technique which allows an areal measurement of surfaces resulting in a high point cloud density. The use of FP as a non-intrusive and fast measurement method in industrial environments has been on the rise.

At the Leibniz Universität Hannover, FP systems have been successfully used within the scope of the collaborative research center (CRC) 489 "Process Chain for the Production of Precision-Forged High-Performance Components". FP is used inside the process chain - as opposed to after the finishing process - since the material surface of the parts is 'optically cooperative' in regards to triangulation techniques.[1] Finished parts, on the other hand, feature glossy non-cooperative surfaces which are hard to measure using FP systems because of the high reflectivity of the surface. The reflectivity leads to either overexposed or underexposed parts of the measurement depending on the projection intensity and the camera exposure.

Though many publications notice the problem of optical cooperativity, few ever deal with solving it. A common camera technique to acquire a wide range of light intensities is called "high dynamic range imaging"

Further author information: (Send correspondence to Omar Abo-Namous)
Omar Abo-Namous: E-mail: omar.abo-namous@imr.uni-hannover.de, Telephone: +49 511 762 4278

Reflection, Scattering, and Diffraction from Surfaces II, edited by Zu-Han Gu, Leonard M. Hanssen, Proc. of SPIE Vol. 7792, 77920V · © 2010 SPIE
CCC code: 0277-786X/10/$18 · doi: 10.1117/12.860647

(HDRI). It includes taking two or more pictures of the same scene but with different exposure times and merging them by excluding under- and overexposed pixels and leveling the different light levels. Typically three images are taken to represent highlevel, midlevel and lowlevel intensities. For a time-sensitive measurement of FP, this would mean at least trippling the time a measurement would take.[2]

Ri et al.[3] suggested a micromirror-based camera setup to extend the dynamic range of individual camera pixels. First a grey image is projected onto the surface and recorded by the camera. Bright pixels on the camera mean a high reflectivity of the corresponding surface area and a potentially overexposed pixel within the measurement, whereas dark pixels could lead to an underexposed pixel. A digital micromirror device (dmd) is positioned such that each micromirror corresponds to a pixel on the camera. By programming the inverted light intensity of the initial recording onto the dmd, the light intensities of each pixel can be normalized such as to extend their dynamic range. Though the method has been successfully used, it comes with the expense of a perfectly aligned dmd and an additional projection at the beginning of any FP measurement.

The industry-related transfer project T5 ("Non-contact geometry inspection of finished rotationally symmetrical work pieces with optically non-cooperative surfaces") within the CRC 489 deals with measuring the surface geometry of finished parts by altering the scattering characteristic of their surface. The definition of optical cooperativity becomes crucial for the purpose of this research.

It should be noted that for different measurement methods different criteria have to be defined. Unless stated otherwise, any further mention of 'optical cooperativity' in this paper refers to FP.

2. OPTICAL COOPERATIVITY

2.1 General Overview

Optical surface measurement systems rely on the light reflected by the surface of the measurement object. Surfaces reflect light differently depending on their material, their surface structure and the wavelength, incident angle and polarity of the light. Major contributors to Optical Incooperativity are:

1. dark materials with very low overall reflection intensities
2. subsurface scattering materials where the surface is not the major reflection source, rather the light is reflected by different layers and particles inside the volume of the material
3. highly glossy surfaces where the light is very unevenly reflected

The most common of these charactersitics with industrially finished parts is the glossiness, since cut and finished metallic parts feature a highly reflective surface. Especially with triangulatory methods the glossiness is a major problem since different surface slopes result in a high variation in scattered light intensities.

2.2 Dynamic Range and Reflectivity

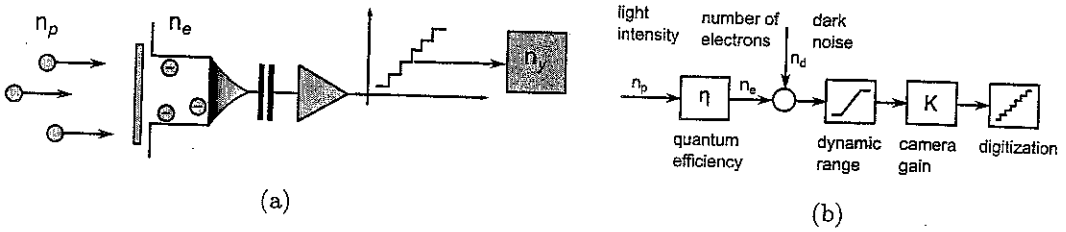

Figure 1. Schematic Figure of a singel pixel in a ccd-camera

Charged-coupled device (ccd) chips feature a dynamic range of light intensities that they can measure in one exposure. This is a result of the transformation process from incident photons to the digital grey value that is encoded in the resulting image. Figure 1 shows the typical setup of a camera pixel. Photons that fall on

the photoactive part of a pixel while the shutter is open cause an accumulation of electric charges within the potential well of the pixel. At the end of a recording sequence the charges are sequentially read out, a camera gain is applied to the voltage after which it is quantized to a grey value usually between 0 and 255.

The size of the potential well within one pixel is of course finite, so that only a maximum amount of electrons can be saved therein. Different chip designs deal differently with additional electrons, but in most cases they spill to neighbouring pixels resulting in either oversaturated smudges or stripes in the recorded image. So, not only does this process result in some information of the affected pixel missing or altered, but the information in the neighbouring pixels is also altered. Ideally the length of the shutter time and / or the size of the aperture should be chosen so that no pixel is oversaturated.

On the other side every camera pixel features a dark current. Dark current denotes the electric charge that accumulates in the potential well of a pixel even if no light falls onto it and is dependant on the temperature of the chip. The minimum amount of photons that can be meaningfully interpreted to represent image information in a camera pixel has to be higher than the amount of photons needed to generate the electrons of the dark current.

The dynamic range defines the ratio between the number of photons that lead to a saturation of a pixel ($n_{p,sat}$) and the minimum amount of photons needed to overcome the dark noise in it ($n_{p,min}$). The dynamic range can also be defined by the respective number of electrons as shown in equation 1.

$$DYN = \frac{n_{p,sat}}{n_{p,min}} = \frac{n_{e,sat}}{n_d}* \tag{1}$$

Optical cooperativity in respect to reflectivity of a surface can be defined to be the proportion between the highest and lowest light intensity being reflected by the surface on one hand and the dynamic range of the camera on the other.

2.3 Bidirectional Reflectance Distribution Function

The Bidirectional Reflectance Distribution Function (BRDF) serves as a method to describe the distribution of the light reflected by any surface. The BRDF can be dependant on many parameters, the basic ones being the incident and scattering angle of the light†, but also including the wave length of the light, its polarity etc.

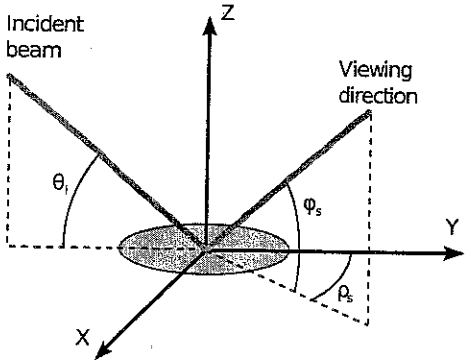

Figure 2. Geometric Parameters of the Bidirectional Reflectance Distribution Function

The surface of a perfect mirror reflects all of the incident light in one direction, which is opposite to the incident angle. In contrast, a lambertian scatterer (named after Johann Heinrich Lambert[5]) reflects in the incident light equally over the hemisphere above it. Any real surface combines both reflection types.

*$n_{e,sat}$ is the saturation potential, whereas n_d is the dark current, all symbols adhere to the EMVA Standard 1288[4]

†θ_i for the incident light and ϕ_s and ρ_s for the scattered light direction. Refer to Figure 2 for details

2.4 Optical Cooperativity and the Surface Profile

A correlation between the surface topography and the light scattering characteristics of the surface is suggested in numerous references.[6] For smooth surfaces (according to the Rayleigh smooth-surface criterion) a bidirectional correlation between the brdf-function and the power spectral density (psd) of the surface topography is possible. Still, for rough surfaces it should be possible to estimate the brdf out of the power spectral density (but not the other way around). One major requirement is that the surface topography behaves like a Gaussian surface, but since industrial finishing processes seldomly create deterministic surfaces unless on purpose, this requirement is met by most surfaces.

We used the c++ library SCATMECH[7] and the corresponding software "Modeled integrated scatter tool" (MIST)[8] to estimate the brdf of different surfaces. Both were developed at the National Institute of Standards and Technology (NIST). We measured the surface topography using a tactile roughness measurement instrument. The psd is defined as the Fourier transform of the autocorrelation function of a signal.

The software package Matlab contains the function `psd`, which automatically calculates the power spectral density of a given signal.

In MIST we used the "Microroughness BRDF Model", which expects the psd either in form of a parametrized function or a table. We used the psd-data in the form of an external file both of untreated polished surfaces and of treated surfaces (see below).

The initial output of the program is a brdf function for a fixed incident angle and a variable scattering angle. Again, the aim is to see whether maximum and minimum scatter within a predefined range fits within the dynamic range of the camera. The dynamic range was obtained from the manufacturer of the camera.

2.5 Surface Treatment Methods

Different surface treatment methods alter the surface structure on a micrometric and submicrometric level. These include mechanical, chemical, electrochemical and physical treatment methods. The employed surface treatment methods are based on expected results and some prelimenray testing on stainless steel.

Table 1. Surface treatment methods that were used to alter the surface structure to make optically more cooperative

Treatment Method	**Parameter ranges used**
Blasting with fused alumina EKF1000	$2-8\ bar$, $5-20\ s$, $5-10\ cm$
PVD etching with argon/nitrogen plasma	2.5 h, HF power $700-1400\ W$
Etching in H_2SO_4 (20 $wt\%$)	$1-15\ minutes$
Electrochemically etching in H_2SO_4 (20 $wt\%$)	$1-5\ minutes$, $1-2\ A/dm^2$ anodic
Electrochemically etching in $1-MHCl$	$1-5\ minutes$, $1-2\ A/dm^2$ anodic
Chemically copper-plating	1 h, various additives
PVD etching with argon/nitrogen plasma	2.5 h, HF power $700-1400\ W$

In table 1 the used surface treatment methods are shown as well as the parameters that were varied for the specific treatment method. All of the methods used here are abrasive, which means that they wear some material off the surface. Additionally, there are a few layering methods by which a thin and optically cooperative layer is distributed on the surface of the measurement object. Ideally the layer is as thin as possible and in any way not thicker than the uncertainty of the measuring system.

Here, we would like to concentrate on the mechanical method of sand blasting.

3. MECHANICAL SURFACE TREATMENT

3.1 Setup and Parameters

The blasting was done using 5 μm fused alumina being blasted at 2, 4, 6 and 8 bar from distances of 5 cm and 10 cm respectively[‡]. As will be shown, the duration of the blasting process mainly affects the stability of the process, since it is rather random. We increased the duration from 10 to 20 seconds. Each surface was polished before treatment and some polished surfaces were preserved for reference measurements.

3.2 Characteristic Values

For determining both the surface structure and the reproducibility of that structure different characteristic values of the surface topography were chosen. The equations for the characteristic values are given here for sampled surfaces only.

Table 2 shows three very common formulas to characterize a surface structure. The arithmetic average R_a is one of the most common surface characteristics. The average peak height over a number s of line segments R_{ti}. Both R_a and R_z are not suitable to be correlated to the optical roughness of a surface. The root mean square R_q is another well-known characteristics and can be utilized to characterize the optical roughness of some surfaces. Figure 2 features the definitions of R_a, R_z and R_q and the values for the polished surface, which were averaged over measurements from 10 different surfaces.

Table 2. Typical characteristic values for surface roughness

Characteristic Value	$R_a = \frac{1}{n}\sum_{i=1}^{n} \lvert y_i \rvert$	$R_z = \frac{1}{s}\sum_{i=1}^{s} R_{ti}$	$R_q = \sqrt{\frac{1}{n}\sum_{i=1}^{n} y_i^2}$
Size in μm	< 0.02	< 0.2	< 0.05

3.3 Reproducibility

To determine the reproducibility of the blasting process, the process was repeated ten times for each parameter set. The pressure was identified to be the main parameter. So characteristic values were drawn as function of the pressure for different sets of the distances between blaster and surface and the blasting duration. Figure 3 denotes the measured arithmetic averages of all surfaces, that were sand blasted for 10 seconds from a distance of 5 cm. The sand blasting pressure was changed between 2 bar and 8 bar. The point of zero pressure has been chosen for referencial purposes as the R_a value of the polished surface. Clearly, the values vary very much. For a pressure of 6 bar the R_a value is scattered between 0.8 μm and 4 μm.

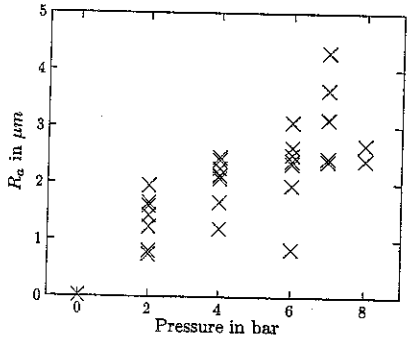

Figure 3. Arithmetic Average of the surface structure of a sand blasted surface (5 cm, 10 sec)

[‡]about 2" and 4"

Equally scattered are the values for the the average peak height R_z and root mean square R_q of the surface which are displayed in figure 4.

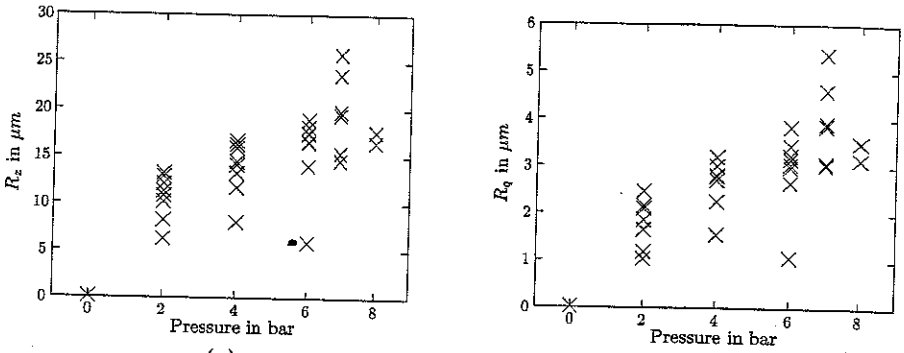

Figure 4. R_z (a) and R_q (b) for treated surface (5cm, 10s and different pressures)

The process is insofar stable as it seems to produce a higher surface roughness with rising blasting pressure. The variance in surface roughness can be minimized by extending the blasting duration and - to a lower extent - by increasing the distance between blasting nozzle and object surface. Figure 5 shows the R_a and R_q values for surfaces, that were blasted from a distance of $15cm$ for 20 seconds. The variance of the characteristic values for each blasting pressure is much smaller for this setup.

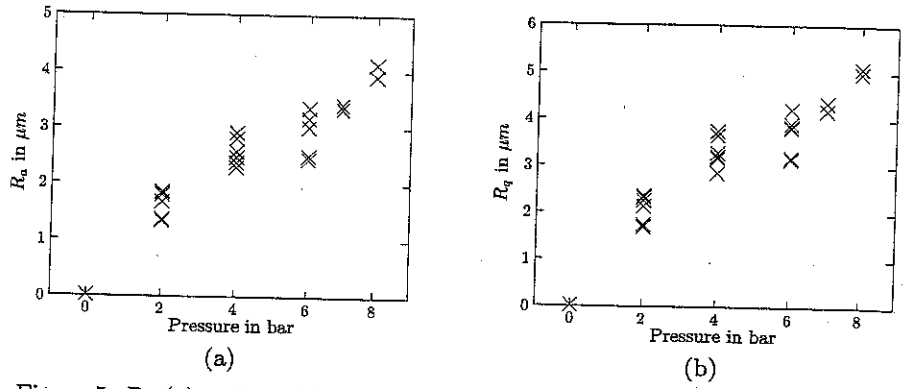

Figure 5. R_a (a) and R_q (b) for treated surface (15cm, 20s and different pressures)

It should be noted that the tuning of the setup parameter was done manually. We are confident that with a stricter control of the measurement setup, a reproducability of less than 1 μm can be achieved.

4. RESULTS

4.1 Topographic Evaluation

Based on 2.4, we used the software MIST to estimate the bidirectional reflectance distribution function of several surfaces that were produced. We worked under the assumption that for all viewing angles where the relationship

$$DYN \geq \frac{max(brdf)}{min(brdf)} \tag{2}$$

is valid, the surface is measureable with at least one set of parameters for projector light intensity and camera shutter time.

For the polished surface, the brdf is shown in figure 6(a). It has a very high peak around the angle of total reflection (30°). The maximum amount of light calculated by MIST at this peak is about 850 times bigger than the highest light intensity value for any viewing angle outside the small angle range around the angle of total reflection. The dynamic range of the camera is about 550, which means that the surface cannot be fully measured using this camera.

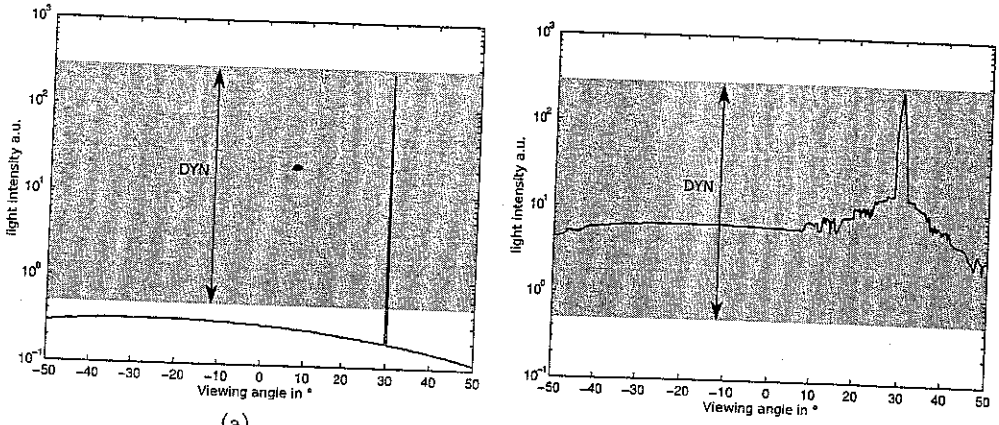

(a) (b)

Figure 6. Brdf of a polished (a) and blasted surface (b)

On the other hand the brdf in figure 6(b) is derived from the surface structure of a surface that has been blasted using 6 *bar* from a distance of 15 *cm* for a duration of 20 *s*. The peak light intensity at 30° viewing angle is only about 35 times higher than the mean light intensity outside the rather big (around $5 - 8°$) total reflection zone. This means that the whole surface can be measured with only one camera shot and there is even a significant range in which the dynamic range (read: the camera shutter time and the light intensity of the projector) can be varied without losing the optical cooperativity.

4.2 Optical Validation

We used an experimental method that uses two planar surfaces with the same surface structure to validate our findings. We used a fringe projection system with a projection angle of $\beta = 45°$. One of the surfaces is positioned evenly, while the other one is tilted by half of the projection angle (see Figure 7(a))[§]. The tilted surface is meant to reflect most of the incident light from the projector directly into the camera. The even surface reflects most of the light away from the camera.

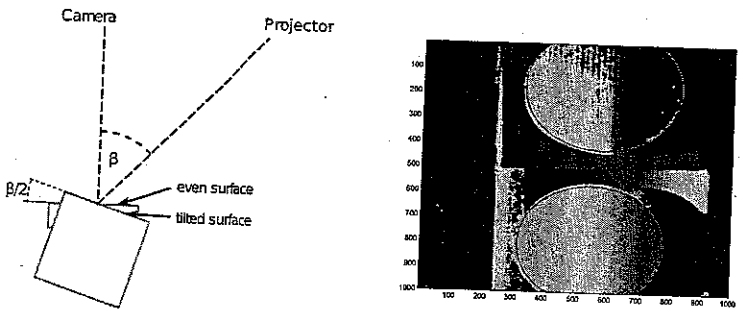

(a) (b)

Figure 7. Measurement setup (a) and example measurement (b)

This way we get in one image the highest light intensity possible and a very low intensity. Figure 7(b) shows one exemplary measurement of the two surfaces which are both framed with a red circle. The dark-blue areas

[§]Both surfaces are positioned relative to the camera plain.

feature the value -10 which in this case means, that they weren't measureable by the fringe projection system at this light intensity. As can be seen, in this example the tilted surface is completely measureable whereas the even surface is only partly measureable A considerable amount of pixels within the even surface did not turn up.

Varying the amount of light intensity of the projector, we would expect to have a very good visibility of the tilted surface using a low intensity and an oversaturation, once the intensity gets higher. The even surface should behave exactly the other way around - with high light intensities it should be very well visible, but with lower intensities the light that is reflected into the camera won't be enough to produce valuable data.

In figure 8 the amount of measureable pixels on the tilted (blue circles) and the even surface (red crosses) are drawn as functions of the light intensity applied. As can be seen in figure 8(a), there is no light intensity range where both polished surfaces can be measured. For low intensities smaller than 1 the tilted surface is measureable, whereas the even surface is only measureable in the light intensity range around 100.

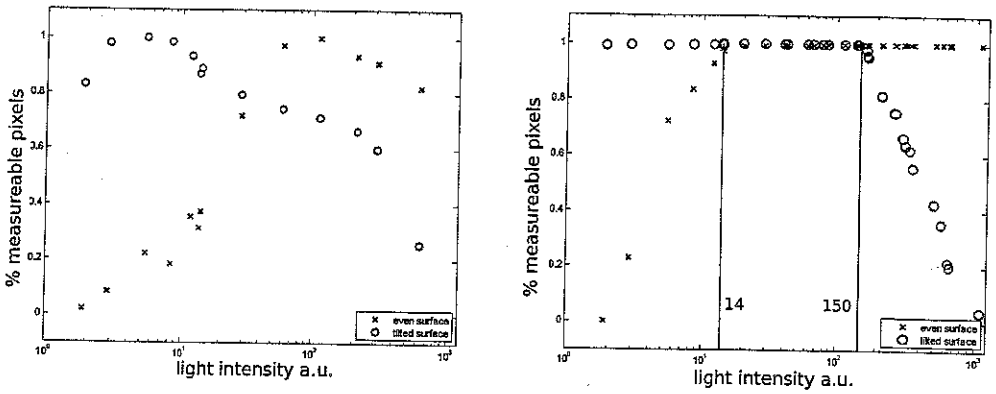

Figure 8. Measurement setup (a) and example measurement (b)

The results for the blasted surface shown in figure 8(b) feature an area between the light intensities 14 and 150, where both surfaces can be completely measured. This of course concurs with the findings of the topographic evaluation.

5. CONCLUSION

It was possible to produce optically cooperative surfaces out of optically incooperative surfaces by applying mechanical surface treatment methods. The process of sand blasting though highly random can be stabilized by increasing the distance between the blasting nozzle and the surface and extending the duration of the blasting process. We found that the resulting surface roughness behaves proportional to the blasting pressure applied. Mechanical surface treatment is destructive to the surface and should therefor be applied with caution if the part in question is not a testing part. As we've shown, there are many more surface treatment methods that can be chosen depending on the specific industrial application. For an inline inspection of production parts, it could be usefull to apply non-destructive surface treatments, which generally put a thin lambertian layer onto the surface.

The evaluation methods applied here vary in the experimental requirements. The optical method used for verification purposes requires two surfaces that are specifically designed for the measurement method. Furthermore it is a rather time intensive measurement depending on the light intensity resolution that is needed. The topographic method requires only a tactile measurement of the surface roughness profile, which can then be fed to the brdf-estimation process.

ACKNOWLEDGMENTS

The authors would like to thank the German Research Foundation (DFG) for funding the project T5 "Non-contact geometry inspection of finished rotationally symmetrical work pieces with optically non-cooperative surfaces" within the CRC 489.

REFERENCES

[1] Kästner, M.; Gillhaus, R. and Reithmeier, E., "Geometry inspection of precision-forged crank shafts based on optical multisensor techniques," *Journal of the CMSC* 4(2), 27–32 (2009).

[2] Reinhard, E., Ward, G., Pattanaik, S., and Debevec, P., [*High Dynamic Range Imaging: Acquisition, Display, and Image-Based Lighting (The Morgan Kaufmann Series in Computer Graphics)*], Morgan Kaufmann Publishers Inc., San Francisco, CA, USA (2005).

[3] Ri, S.; Fujigaki, M. and Morimoto, Y., "Intensity range extension method for three-dimensional shape measurement in phase-measuring profilometry using a digital micromirror device camera," *Appl. Opt.* 47, 5400–5407 (Oct. 2008).

[4] "Emva standard 1288, standard for characterization and presentation of specification data for image sensors and cameras." http://www.emva.org/.

[5] Lambert, J. H., [*I.H. Lambert Photometria, sive, De mensura et gradibus luminis, colorum et umbrae [microform]*], V.E. Klett, Augustae Vindelicorum : (1760).

[6] Stover, J. C., [*Optical Scattering - Measurement and Analysis*], SPIE Optical Engineering Press (1995).

[7] Germer, T. A., "Scatmech: Polarized light scattering c++ class library." http://physics.nist.gov/scatmech.

[8] Germer, T. A., "Modeled integrated scatter tool (mist)." http://physics.nist.gov/scatmech.